

INVESTIGATION OF LONGWALL FACE VENTILATION AIR-SPLITTING METHODS FOR IMPROVED DUST CONTROL

J. A. Organiscak
NIOSH
Pittsburgh, PA

ABSTRACT

Two types of airflow splitting methods for improving longwall dust control were investigated by NIOSH's Pittsburgh Research Laboratory. These methods included a translucent mesh barrier and a staged spray barrier system to confine the shearer-generated dust to the coal extraction side of the longwall face while maintaining a cleaner split of airflow on the opposing worker walkway side of the longwall face. The translucent mesh barrier was shown to provide notable dust control effectiveness up to 60 m downstream of the shearer in both the laboratory experiments and a longwall field evaluation, provided the mesh barrier remains relatively parallel to the airflow. The staged spray barrier system showed marginal dust control effectiveness in the laboratory and subsequently was not field tested.

INTRODUCTION

Ventilation is a key element in controlling airborne respirable dust (ARD) generated at longwall mining operations. Ventilation is primarily used for diluting and removing ARD generated from coal extraction at the mining face. Prior studies have shown that an indirect relationship exists between the amount of ventilation and dust concentrations measured at the longwall face (Haney et al. 1993; and McClelland et al., 1987). However, there are both practical and economic limits to the air quantity that can be delivered by the mine ventilation system to the longwall face.

A significant portion of a mine's fan(s) capacity is lost or short-circuited in the ventilation system before it reaches the mining face. Air leakage from the intake to the return air courses usually occurs through the ventilation control devices constructed throughout the mine. These include stoppings, doors, overcasts, etc. between the intake and return entries of the mine. These control devices leak because of stress-induced entry deformation, physical deterioration with time, and/or construction quality. Mine ventilation systems are considered to be efficient if they can deliver 50% of its fan(s) quantity to the working face(s) (Bise, 1986). Mine

ventilation also has economical limitations placed on it because the power used to deliver a unit quantity of air increases by a cubic relationship with quantity.

Although ventilation is one of the most important elements of longwall dust control, additional control methods are needed to assist with the reduction of high dust concentrations in localized areas of the mining face. The single largest longwall dust source is the shearing machine cutting coal along the entire longwall mining face (Colinet et al., 1997; Jankowski et al., 1991; and Jankowski and Organiscak, 1983). The worker walkway on the gob side of the longwall face becomes contaminated with dust adjacent to and downstream of the shearer (Ruggieri et al., 1983). Employees working in these areas adjacent to and downstream of the shearer are commonly exposed to the highest dust concentrations at the mining face.

Research has been conducted to reduce the dust contamination of the worker walkway near and downstream of the shearing machine. Concepts that were studied included shearer-mounted water spray air movers, physical barriers mounted on the shearer, ventilation curtains mounted along the face, and support-mounted compressed air spray movers. The shearer-clearer water spray system was one of the most successful developments of these dust control concepts and is used by more than 80% of the U.S. longwall operators (Haney, 1995). This shearer-mounted external spray system uses 10 external hollow cone nozzles directed with the ventilation airflow over the shearer body and has physical barriers mounted between the cutting drums and worker walkway from splitter arms attached to the machine. This system confines the shearer dust to the mining face away from the shearer operators and has been shown to provide up to 50% reduction in dust (Ruggieri et al., 1983; Jayaraman et al., 1985). However, the air-splitting effectiveness of the shearer-clearer diminishes downstream of the shearer, especially at the highest water spray pressure tested (1,724 kPa).

Several ventilation curtain concepts have been found to be either ineffective or impractical for air-splitting at longwall operations. One concept was to increase the air velocity over the shearer and face

conveyor by placing brattice curtains across the workers walkway to decrease longwall entry area (Babbitt et al., 1990). Various curtain spacings (4.6, 7.6, and 12.2 m) arranged at perpendicular and 45° orientations with the airflow were studied in a full-scale longwall ventilation gallery with a tracer gas. Although the curtains increased face air velocity, the eddy air currents produced downstream of these curtains allowed contaminated face air to be drawn into and linger in the walkway. The best walkway conditions were the baseline tests without any curtains. Another more effective ventilation curtain concept studied in the full-scale longwall gallery was an extended face conveyor spill plate (curtain barrier) between the face area and worker walkway (Babbitt et al., 1990). Laboratory tests showed that a fully extended face conveyor spill plate or curtain to the roof improved the air quality in the worker walkway downstream of the shearer. However, this type of barrier would impede worker visibility of the extraction face and would not be practical for longwall operations.

A compressed air spray movement system mounted on longwall supports was another air-splitting dust control concept studied in a full-scale longwall gallery. Four compressed air sprays were mounted on every longwall support location. Two sprays were directed from the support canopy 45° downward with the airflow toward the face conveyor, and two sprays were directed from the worker walkway 45° with the airflow toward the face. Eighty nozzles were placed on a 30.5-m section of face area comprising about 20 supports. Tracer gas testing showed that the compressed spray air system provided greater than 60% reduction in tracer gas levels measured in the worker walkway next to the shearer at air velocities of 1.0 and 1.5 m/sec. At higher air velocities of 2.0 and 2.8 m/sec, the system's performance diminished to about 50%. Although this compressed air system displayed good performance, it required a 183-kW, high-capacity compressed air supply for the 59.5 m³/min delivered along the 30.5-m section of the longwall gallery, diminishing its practicality for underground use.

Because the extended spill plate barrier and support-mounted directional spray system concepts showed promise for effective longwall dust control, additional full-scale laboratory tests were conducted on more practical engineering control applications of these ventilation concepts. A translucent mesh barrier was examined to provide a compromise between airflow containment and visual transparency. A staged spray barrier method was also studied to provide air-splitting with a less complex spray system. Both of these air-splitting methods were studied at NIOSH's Pittsburgh Research Laboratory for potential longwall mining application. This report describes the research into their design parameters and related dust control effectiveness.

TRANSLUCENT MESH BARRIER

A translucent mesh barrier placed along the longwall face was devised to create two separate splits of airflow between the extraction face and worker walkway while providing some worker visibility through the barrier. Specific details of the investigation into this longwall dust control method have been published (Organiscak and Leon, 1993) and will be summarized in part in this report. This investigation encompassed experimental studies at NIOSH's Lake Lynn Laboratory and one field study at an operating longwall. A more rigorous statistical analysis of the laboratory and field data was recently conducted and is included as part of this report.

Lake Lynn Laboratory Experiments

Experiments were conducted at Lake Lynn Laboratory to study the key dust control parameters involved in the application of the translucent mesh partition. These key factors included the downstream distance from the dust source, mesh porosity, and air velocity. The air-splitting abilities of three polyester mesh-type fabrics compared with baseline conditions of no mesh were studied at four air velocities along a narrow 183-m test entry section of the Lake Lynn Experimental Mine. The characteristics of these polyester mesh fabrics were notably different and are shown in Table I. The mesh types tested ranged from the most porous fabric of 84% open area to a tighter fabric of 30% open area. The weight and strength of the mesh fabrics shown in the table were indirectly related to the open area of the fabric.

Table I. Characteristics of mesh types studied in the laboratory (from Organiscak and Leon, 1993).

MESH TYPE	A	B	C
Fabric Material	Polyester	Polyester	Polyester
Opening Size, mm	6.4	3.2	1.6
Mesh Count, holes/cm ²	1.4 × 2.0	1.8 × 3.5	3.1 × 3.9
Mesh Porosity, %	84	52	30
Thickness, mm	0.05	0.10	0.13
Weight, g/m ²	159	214	365
Ball Burst, kPa	1,380	2,070	3,790

Figure 1 shows the experimental layout of the mine entry test section. The test entry section was narrowed from 5.5 to 2.4 m by constructing a 183-m wood-framed brattice curtain wall 2.4 m from one side of the entry wall to simulate a realistic cross-sectional area of an average U.S. longwall face. A 152-m-long continuous section of each mesh fabric was hung from the

roof to the floor in the middle of the test entry (1.2 m from the entry wall and the brattice wall). Baseline tests were also conducted without any mesh to measure the natural dust migration across the test section entry. Air velocity down the test section was controlled by a brattice curtain regulator positioned across the beginning of the adjacent parallel air split, opposite the test section. Baseline and mesh testing experiments were conducted under four different air velocities of 1, 2, 3, and 4.1 m/sec, repeated three times under each test condition. Absolute random sampling of the test conditions was impractical, because mesh replacement was very labor-intensive. However, a moderate mix of the test conditions was achieved by testing different air velocities for each type of mesh, changed out several times throughout the total experimental period.

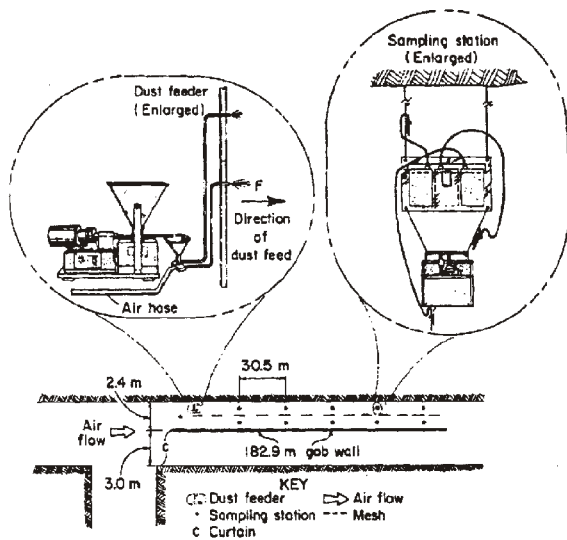


Figure 1. Lake Lynn experimental setup (from Organiscak and Leon, 1993).

Airborne respirable dust (ARD) sampling was conducted on each side of the test section entry at distances of 30.5, 61, 91.5, 122, and 152.5 m downstream of the dust source for each test condition. Three gravimetric ARD personal dust samplers and one Real-Time Aerosol Monitor (RAM-1)¹ were located at each sampling location. The personal dust samplers used a Dorr-Oliver 10-mm nylon cyclone classifier operated at 2 L/min. The three personal samplers at each sampling location were spaced at uniform distances between the roof and floor. The average ARD concentrations of the three personal samplers for each sampling location were used in the data analysis. The RAM-1 samplers were only used to ensure uniform dust concentrations during each test. A sampling station was also located upstream of the test entry section to ensure that a good quality of ventilation air was used for each test.

Airborne dust was generated on the mine wall side of the entry with a Vibra Screw SCR-20 feeder supplying Keystone Filler and Mfg. Co.'s Mineral Black # 325BA dust into a compressed air dispersion system. The dispersion system discharged dust at equal distances from the roof and floor on the mine wall side of the entry. The dust feed rate was adjusted for air quantity to maintain a similar dust concentration for each test so that the effect of air velocity on air-splitting could be more clearly studied. Test duration was 65 min. A total of 48 valid tests were conducted for the various mesh configurations at different air velocities.

Experimental Results

ANOVA analysis was conducted on the experimental raw data to examine the significance of the controlling factors on mesh barrier air-splitting. The dependent variable was the dust concentration on the off-feeder side of the entry. The independent variables were the downstream sampling distance, the barrier porosity, and the entry air velocity. The average dust concentration across the entry (for both sides) at each downstream sampling distance was used as the covariate for the dependent variable. The numerical results from this analysis are shown in Table II. The graphical results are shown in Figure 2.

¹ Mention of any company name or product does not constitute endorsement by the National Institute for Occupational Safety and Health.

Table II. ANOVA analysis of mesh experiments.

VARIATION SOURCE	SUM OF SQUARES	DEGREES OF FREEDOM	MEAN SQUARE	F-RATIO	SIGNIFICANCE LEVEL
COVARIATE					
Entry Dust Concentration	277.43	1	277.43	1000.00	0.000
MAIN EFFECTS					
Downstream Distance	195.18	4	48.80	332.21	0.000
Barrier Porosity	175.54	3	58.51	398.36	0.000
Air Velocity	5.10	3	1.70	11.58	0.000
INTERACTIONS					
Distance-Porosity	17.60	13	1.35	9.22	0.000
Distance-Velocity	6.49	13	0.50	3.40	0.001
Porosity-Velocity	12.47	9	1.39	9.44	0.000
RESIDUAL	28.64	195	0.15		

All of the independent and covariate variables significantly impacted the dust concentrations on the off-feeder side (walkway) of the entry. The two independent variables with the largest effect were the barrier porosity and downstream distance from the dust source (see Table II and Figure 2). Figure 2 shows that the walkway dust concentration directly increases with the downstream distance from the dust source. This figure also shows that a lower mesh porosity significantly reduces the walkway dust concentrations and increases the downwind distance for comparable dust concentrations. Because the dust feed was adjusted for air quantity to maintain similar dust concentrations during each test, the air velocity had the least effect on the dust concentrations on the off-feeder side of the entry (see Table II).

The relative dust control efficiency of each mesh type was also examined for its practical application on longwall operations. Dust control efficiencies for each mesh at the various downstream locations were determined as the percent change in walkway dust concentrations with respect to the baseline tests, without the mesh barrier. The average walkway dust concentrations at each downstream sampling location for the mesh tests were first adjusted or normalized by a factor that equated the average entry dust concentrations at each location (both sides of the entry) of the mesh tests to the baseline tests. These adjusted or normalized walkway dust concentrations were then used to determine the percent dust reductions achieved over the baseline tests.

Dust control efficiencies of each mesh type with respect to downstream sampling location are shown in Figure 3. Each dust efficiency curve in Figure 3 represents an average for all of the air velocities tested. Mesh dust control efficiencies were indirectly related to both porosity and downstream distance. Mesh C, which had a 1.6-mm mesh opening size and 30% fabric porosity, reduced dust levels by 79% and 55% at the 30.5-m and 61-m downstream sampling locations, respectively. Mesh B, which had a 3.2-mm mesh opening size and 52% fabric porosity, reduced dust levels by 58% and 36% at the 30.5-m and 61-m downstream sampling locations, respectively. Mesh A, which had 6.4-mm mesh opening size and 84% fabric porosity, showed little improvement over the baseline conditions for all of the downstream sampling locations. These results indicate that mesh fabrics for longwall application need a porosity of about 50% or lower for efficient dust control. However, as the mesh porosity or hole size is decreased, visibility through the mesh fabric is reduced.

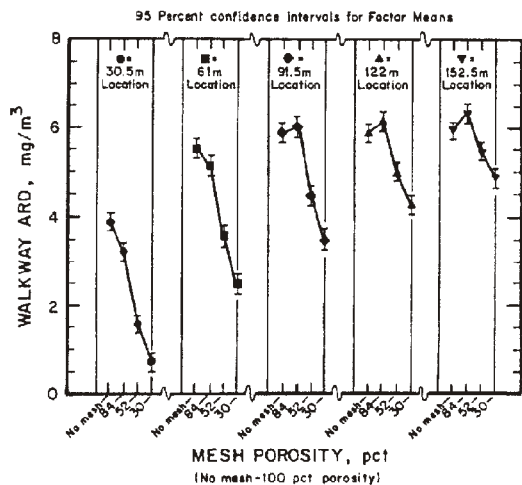


Figure 2. Experimental mean plots of walkway dust concentrations versus mesh porosity and downstream distance.

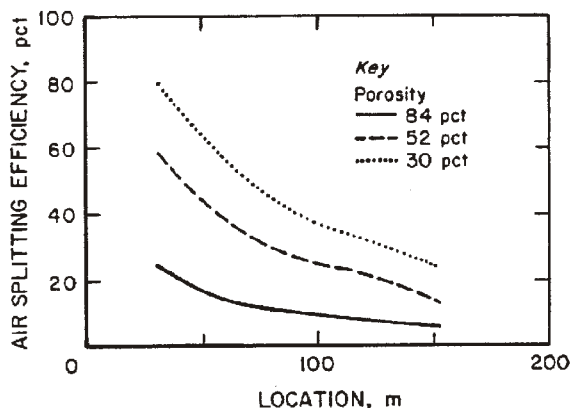


Figure 3. Downstream air-splitting efficiency relationships for the mesh barriers tested.

Longwall Field Study

One longwall field study was conducted using Mesh Type B as the air-splitting barrier. This mesh type was preferred by the longwall operator as a functional compromise between worker visibility and dust control efficiency. A continuous roll of fire-retardant polyester mesh fabric of type B was obtained for this underground study. Four samples of this mesh were subjected to a Flammability Test (ASTM E-162, 1996) and were classified as a low-risk fire hazard ("Class A") under the flame spread classification system.

The longwall operation extracted a 3.7- to 4.3-m-thick, high-volatile bituminous coal seam along a 225-m-wide mining face. Methane emission at this mine was historically low, reducing the potential for methane

accumulation hazards along the face during the mesh air-splitting tests. This longwall operation used a unidirectional cutting sequence, with a radio remote-controlled shearer cutting in the head-to-tail direction and cleaning up in the tail-to-head direction. Radio remote-control operation of the shearer from the worker walkway was crucial for operation with the mesh barrier. The supports were advanced on the tail-to-head cleanup pass.

The mesh was continuously hung along a 140-m section of the face, from longwall supports 4 through 95, to separate the worker walkway from the extraction face (see Figure 4). The mesh was hung from the canopy of each support by rods bolted to the underside of the face lighting fixtures. Surgical latex tubing was attached between the rods on the shields for continuous hanging of the mesh. Additional mesh material was folded on the tubing between the supports to accommodate support movement. Cap lamps were mounted on the shearer and directed toward the cutting drums to improve the shearer operators' visibility of the mining activities through the mesh. However, the shearer operators still experienced poor visibility through the mesh, requiring more background lighting than that provided by the cap lamps.

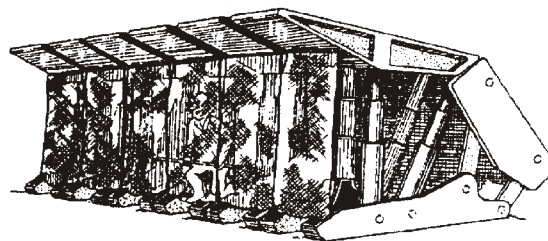


Figure 4. Mesh barrier hung from longwall supports (from Organiscak and Leon, 1993).

Respirable dust sampling was conducted in the worker walkway for several shifts with and without the mesh barrier to evaluate its dust control efficiency. Respirable dust sampling was conducted with the same personal gravimetric dust samplers used in the laboratory study. Four personal dust samplers were worn by research personnel; two samplers were operated during the head-to-tail cut pass and two samplers were operated during the tail-to-head cleanup pass. Research personnel followed the coal extraction process at mobile sampling positions 15 m outby (upstream), 30 m inby (downstream), and 60 m inby the shearing machine. Vane anemometer measurements were also made over the face conveyor and in the worker walkway (both sides of mesh) along the longwall face. Two shifts of control data were collected with the mesh; three shifts of baseline data were collected without the mesh. The average face air velocities between the mesh tests and baseline tests were very similar at 1.56 m/sec and 1.57 m/sec, respectively, making these underground control test conditions comparable.

Field Study Results

The longwall dust data were analyzed for statistical significance by the T-test statistic; results are shown in Table III. The T-test hypothesis for the mean dust concentration difference between test conditions was equal to zero, with the alternative hypothesis being a lower dust concentration for the mesh test condition. Statistical significance was determined for each sampling position by the one-tailed T-statistic. A significant result for this hypothesis testing is at the 95% confidence level or 5% significance level.

The longwall field study verified that significant walkway dust reductions can be achieved downstream of the shearer when the mesh barrier is maintained parallel

to the ventilation airflow. The test results show that the mesh barrier significantly reduced the walkway dust concentrations by 53% and 45% at 30 m and 60 m inby (downstream) the shearer, respectively, during the head-to-tail cut pass. No significant dust reductions at these inby locations were observed for the tail-to-head cleanup pass. The key difference between these shearing directions was the support movement activities for the tail-to-head cleanup pass. Support movement during this pass formed an irregular step in the mesh barrier, altering face airflow movement through the mesh into the worker walkway (see Figure 5). Therefore, mesh barrier continuity along the longwall face is a key aspect for controlling dust downstream of the shearer.

Table III. Longwall mesh test results.

SAMPLE LOCATION AROUND SHEARER	MESH N • 2 shifts		BASELINE N • 3 shifts		ONE-TAILED T-STATISTIC	SIGNIFICANCE LEVEL
	Average mg/m ³	Variance	Average mg/m ³	Variance		
15 m OUTBY						
Head-to-Tail Pass	1.04	0.12	1.37	0.02	• 1.559	0.108
Tail-to-Head Pass	1.28	0.63	1.36	0.02	• 0.178	0.435
30 m INBY						
Head-to-Tail Pass	1.45	0.24	3.09	0.07	• 4.989	0.008
Tail-to-Head Pass	5.48	0.57	5.47	0.43	0.008	0.503
60 m INBY						
Head-to-Tail Pass	1.95	0.12	3.52	0.07	• 5.902	0.005
Tail-to-Head Pass	5.96	0.12	5.38	3.40	0.421	0.649

H₀: (Mesh Average - Baseline Average) • 0

H_a: (Mesh Average - Baseline Average) < 0

STAGED SPRAY BARRIER SYSTEM

A staged spray barrier system along the longwall face was also designed for creating two separate splits of air downstream of the shearer. The objective of this study was to develop and test a much simpler and more functional air-induced spray system compared to past support-mounted spray systems. This spray system involved mounting several flat fan spray nozzles vertically onto a physical barrier (conveyor belting) and spacing these barriers at equal distances with the airstream. Preliminary testing was conducted for several water spray nozzle arrangements and barrier distances. A two-phase air-atomized staged spray barrier system was further tested at various spray and ventilation operating parameters. The tests were conducted in NIOSH's Safety

Research Coal Mine at the Pittsburgh Research Laboratory (PRL).

Preliminary Staged Spray Barrier System Development

Preliminary tests were conducted with water sprays mounted on physical barriers to separate entry airflow for a 30.5-m distance in the Safety Research Coal Mine at PRL. A 122-m-long, 0.9-m-high barrier was constructed out of lumber and brattice cloth to simulate a longwall face conveyor spill plate. This barrier was positioned approximately along the center of a 3.0-m-wide straight section of entry. For the initial spray layout tests, four water spray manifolds were vertically mounted on 1.2-m by 1.2 m pieces of conveyor belting and were hung above and nearly parallel (• 5° orientation with the airflow) to the mock spill plate barrier on 7.6-m centers

(see Figure 6). Each spray manifold had three equally spaced nozzle locations, oriented parallel to the belt barrier, and was placed on the dust generation side of the mock spill plate and belt barriers. The preliminary air-splitting tests examined several spray nozzle sizes, spray manifold layouts, and spray operating pressures at several air velocities (see Table IV). A Cat Pump with an adjustable pressure regulator was used to provide different water spray pressures. Air velocities in the entry were controlled by changing the mine's fan speed (three-speed fan).

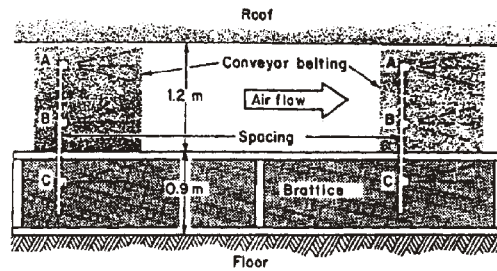


Figure 6. Walkway side view of staged spray layout.

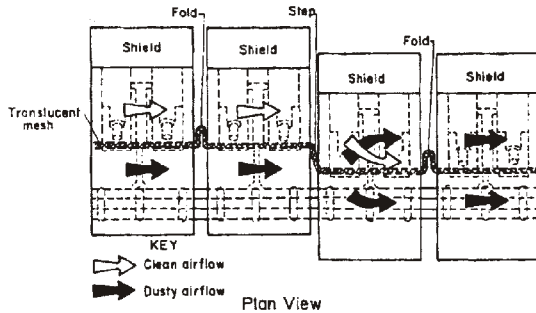


Figure 5. Underground support movement displacement of mesh (from Organiscak and Leon, 1993).

Dust sampling was conducted 30.5 m downstream of a Vibra Screw SCR-20 dust feeder on the opposing entry side of this dust source (walkway side). Three pairs of personal samplers were equally spaced from the top height of the mock spill plate (barrier) to the roof in the center portion of the walkway side of the entry. Half of these vertically spaced dust sampler pairs were used to measure ARD concentrations with the sprays operating; the other half were used to measure ARD concentrations without the sprays operating. The baseline and spray sampling segments of a test were 20 min each. A RAM-1 was also at this sampling location for real-time examination of dust levels, recorded on a strip chart recorder upstream of the dust feeder. Dust testing was supplemented with visual smoke tests to identify airflow disruptions during this preliminary phase of development.

The preliminary staged spray barrier layout tests conducted are shown in Table IV. Most of this testing was completed at manifold spacings of 7.6 m, water pressures of 689 and 1,379 kPa, and air velocities of about 1.4 m/sec. The ARD results reported are averages of two tests for each condition, except for the 15.2-m manifold spacing for which only one test was conducted at each condition. The very first tests conducted with the H1/4VV2504 flat fan spray nozzles, mounted 38 mm away from the conveyor belt, showed poor dust control efficiency. Two nozzles used in each manifold provided slight increases or virtually no change in walkway ARD levels. Visual smoke examination of these initial staged spray barrier tests showed that operating the two sprays (sprays A and B) above the spill plate barrier allowed the airflow below these sprays to lag and swirl over the spill plate barrier. Placing one of the sprays below the spill plate barrier (sprays A and C) reduced this visual airflow lag; operating all three nozzles (sprays A, B, and C) showed some improvement in the walkway ARD levels. Smoke testing also showed that orienting the staged spray barrier system more than at a slight angle ($\sim 5^\circ$) with the primary ventilation increased eddy currents and airflow migration across the entry.

The most noticeable improvements in ARD walkway levels were achieved when the spray nozzles were moved farther away from the belt barrier. Two H1/4VV2504 spray nozzles seemed to provide the best dust reductions at the same water pressures when these nozzles were moved 102 mm from the belt barrier. A water pressure reduction with the two nozzles showed a notable reduction in dust control efficiency. When the larger H1/4VV2506 nozzles were used, entry air velocity had to be increased to achieve similar results to the smaller nozzles operating at lower air velocities. Increasing the manifold spacing from 7.6 m to 15.2 m with these larger nozzles at the higher air velocity noticeably diminished dust control performance. From these test results seemed that optimum performance of a staged spray barrier system occurred in a limited range of spray manifold and air velocity parameters.

The performance range of the staged spray barrier system was examined by the relative fluid power ratio between the spray nozzles and ventilation airflow. Sprays move air through momentum transfer of the kinetic energy of the spray droplets discharged into the

surrounding environment. Fluid energy applied by these sprays on airflow through a test section of entry can be reasonably determined by using the Bernoulli equation for steady-state flow processes with irreversible losses determined by the Darcy-Weisbach equation. Time usage of this fluid energy is the power expended by each system (spray and ventilation). Mine applicable water, compressed air, and ventilation fluid flow equations are shown in the appendix and can be also found in (Bise, 1986; Hartman, 1961). Mine entry friction factors are also found in these references, and a straight, moderately obstructed sedimentary mine airway friction factor ($K = 60 \times 10^{-10}$) was used for all of the ventilation power determinations. Spray-to-ventilation power ratios were

determined for the more effective tests of sprays located 102 mm from the belt barrier, with the barriers spaced equally at 7.6 m.

Figure 7 shows the spray-to-ventilation power ratio results for the two nozzle types operated at various water pressures and air velocities. The power ratio variations for the same nozzle type and arrangement were accomplished by altering the water pressure or air velocity. Optimum dust control seemed to be achieved with a spray-to-ventilation power ratio between 15 and 30 for these preliminary water spray tests. Dust control efficiency decreased below or above this power ratio range.

Table IV. Preliminary staged spray design testing.

TEST	MANIFOLD SPACING m	SPRAY LAYOUT	WATER PRES kPa	WATER FLOW L/min	AIR VELOCITY m/sec	CHANGE IN ARD LEVELS %
H1/4VV2504 Nozzles 38 mm Away from Belt	7.6	A, B	1,379	27.0	1.3	5% Increase
		A, C	1,379	27.0	1.4	3% Increase
		A, B, C	1,379	40.4	1.4	24% Decrease
H1/4VV2504 Nozzles 102 mm Away from Belt	7.6	A, C	689	19.1	1.4	13% Decrease
			1,379	27.0	1.4	46% Decrease
		A, B, C	1,379	40.4	1.5	32% Decrease
H1/4VV2506 Nozzles 102 mm Away from Belt	7.6	A, C	689	28.8	1.5	30% Decrease
			1,379	39.4	1.4	30% Decrease
			1,379	39.4	2.0	44% Decrease
	15.2	A, C	1,379	19.7	2.0	13% Decrease
			2,068	24.2	2.0	13% Decrease

A key observation was that similar dust control efficiencies were achieved for three smaller H1/4VV2504 nozzles per spray manifold compared to two larger H1/4VV2506 nozzles per spray manifold, delivering nearly the same power ratio. This was accomplished at

the same water pressure and nearly the same water flow rate for these nozzle types (see Table IV). Using a larger spray nozzle reduces the likelihood of orifice plugging from particulate matter in the water supply.

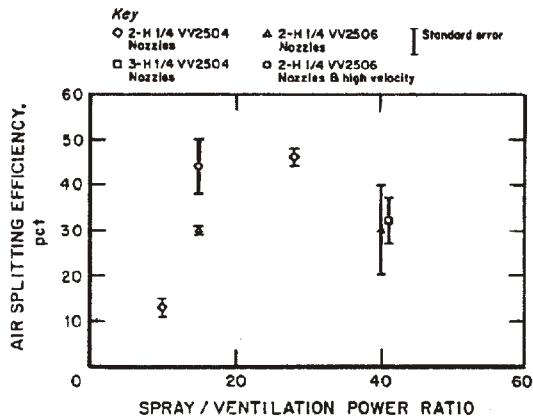


Figure 7. Preliminary water spray-to-ventilation power ratio relationship with air-splitting efficiency.

Although the initial design of a staged spray barrier system was shown to be relatively effective in controlling dust along a short section of entry, the water quantity needed for operating a larger system along a longwall face would most likely be impractical. During these preliminary tests, between 27.0 and 40.4 L/min of water was required to notably control dust along a 30.5 m section of entry. Longwall operations with face lengths typically greater than 180 m would require substantial quantities of water to operate a staged spray barrier system along the face. Spacing the spray barriers at the greater distances reduces water consumption, but also reduces control efficiency. Several tests conducted with water spray barriers spaced at 15.2 m showed marginal dust control efficiency. To reduce the water consumption of the staged spray barrier concept, further laboratory experimentation was conducted with two-phase air-atomized nozzles to investigate their capabilities for air-splitting. These tests also examined dust control effectiveness at greater distances from the dust source.

Two-Phase Air-Atomized Experiments

The staged spray barrier system laboratory testing was continued with two-phase air-atomized nozzles over a longer entry distance. For these tests eight more spray manifold/conveyor belt barrier units were placed over the mock spill plate on 7.6-m centers along the test section entry from 30.5 to 91.5 m downstream of the dust source. The best spray layout identified from the preliminary water sprays tests was used for these air-atomized spray nozzle tests. This spray nozzle layout was the flat fan nozzle positioned above and below the mock spill plate (spray locations A and C), located 102 mm away from the conveyor belt barrier (see Figure 6 and Table IV).

Spraying Systems' 1/4JSUN23 flat fan air-atomizing nozzles were tested at various operating pressures and entry air velocities. A two-level factorial design of the experiments was followed. The experimental design and operating factors are shown in

Table V. These nozzles were operated at compressed air and water pressures within the manufacturer's recommended range. The quantities of water used by these air-atomized spray nozzles were substantially reduced for a staged spray barrier coverage of 91.5 m entry length as compared to water sprays. However, compressed air is also required to operate these air-atomized spray nozzles.

Dust sampling was conducted at 15.2, 30.5, 61, and 91.5 m downstream of a Vibra Screw SCR-20 dust feeder on the opposing entry side of this dust source (walkway side). Three pairs of personal samplers were equally spaced from the top height of the mock spill plate (barrier) to the roof in the center portion of the walkway side of the entry. Half of these vertically spaced dust sampler pairs were used to measure ARD concentrations with the sprays operating; the other half were used to measure ARD concentrations without the sprays operating. The baseline and spray sampling segments of a test were 30 min each. The experiments were randomly conducted; each test condition (trial) was repeated six times. Half of these trials were performed with the sprays operating at the end of the test; the other half, with the sprays operating at the beginning of the test. A RAM-1 was also at the 30.5-m sampling location for real-time examination of dust levels, recorded on a strip chart recorder upstream of the dust feeder. One personal dust sampler was also located upstream of the test entry section to ensure that a good quality of ventilation air was used for each test. Thirty valid tests were completed for the various test conditions.

Table V. Two-level factorial design of air-atomized spray barrier system.

TRIAL	AIR VELOCITY		SPRAY OPERATING PARAMETERS				
	Code	Velocity m/sec	Code	Compressed Air		Water	
				Pressure kPa	Quantity m ³ /min	Pressure kPa	Quantity L/min
1	Low	0.9	Low	207	1.2	138	5.2
2	High	2.0	Low	207	1.2	138	5.2
3	Low	0.9	High	483	2.9	414	14.7
4	High	2.0	High	483	2.9	414	14.7
5	Medium	1.4	Medium	345	2.0	276	10.8

Experimental Results

ANOVA analysis was conducted on these experimental data to examine the significance of the air-atomized stage spray barrier system to split entry airflow. The dust reduction efficiency for each test was the dependent variable. The independent variables were the downstream sampling distance, spray operating pressure, and air velocity. Initial ANOVA results indicated that these independent variables had confounding effects on dust reduction. These confounding effects were due to inconsistent dust control efficiencies measured between the test conditions at the various downstream sampling locations. Figure 8 shows the average dust reduction efficiencies measured along the entry for each test condition. This graph shows that the staged spray barrier system performed better at the low and medium air velocities than at the higher velocity up to the 30.5 m downstream location. Farther downstream of the 30.5 m location the performance was marginal and inconsistent between test conditions. It also seemed that this air-atomized spray system had a limited performance range similar to that of the water spray system.

The performance range of this air-atomized staged spray barrier system was also analyzed by the relative fluid power ratio between the spray nozzles and ventilation airflow. Spray-to-ventilation power ratios were determined for each test condition. Compressed air, water, and ventilation flow equations used to determine power usage can be found in the appendix (Bise, 1986;

Hartman, 1961). ANOVA analysis of the dust control efficiencies with respect to the power ratio and downstream distance from the dust source was conducted; results are shown in Table VI. These results show that the downstream distance had the largest effect on dust reduction efficiencies provided by the staged spray barrier system. Although the power ratio effect showed significance at the 95% confidence level, its overall effect was small in comparison to the other experimental variations.

Interactions between the power ratios and the downstream distances on dust control efficiency can be seen in Figure 9. The dust control efficiency and power ratio relationship noticeably vary for the different downstream sampling locations. The dust efficiency increases with the power ratio at the 15.2-m location. At the 30.5-m location, the optimum efficiency occurs in the middle of the test conditions, similar to the water spray tests at the 30.5-m location. Further downstream, the dust control efficiencies become negligible with inconclusive power ratio relationships. Due to the marginal downstream performance of the staged spray barrier system in the laboratory, underground testing of this system was not pursued.

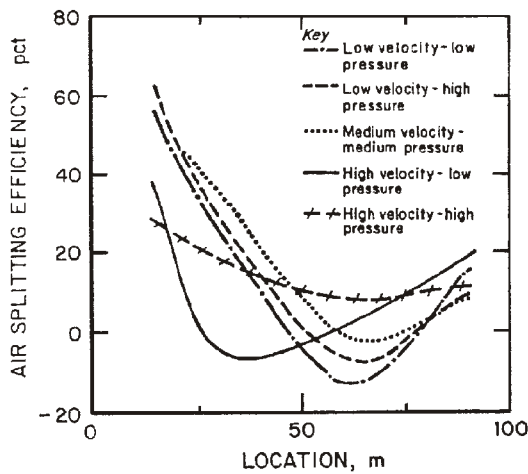


Figure 8. Downstream air-splitting efficiency of air-atomized sprays.

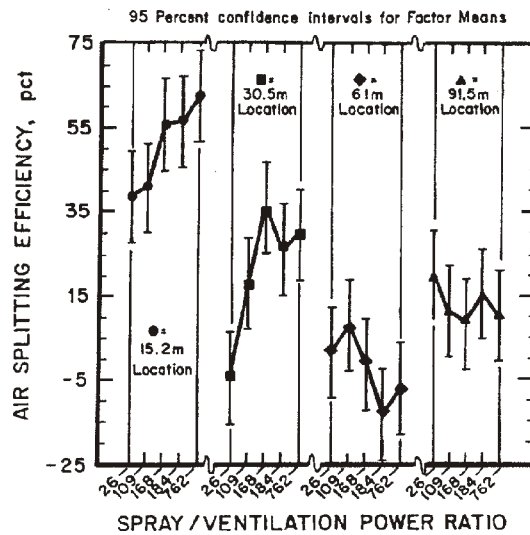


Figure 9. Mean plots of air-splitting efficiency versus spray-to-ventilation power ratio and downstream distance.

Table VI. ANOVA analysis of air-atomized staged spray barrier experiments

VARIATION SOURCE	SUM OF SQUARES	DEGREES OF FREEDOM	MEAN SQUARE	F-RATIO	SIGNIFICANCE LEVEL
MAIN EFFECTS					
Downstream Distance	44,672.54	3	14,890.84	82.21	0.000
Power Ratio	1,809.04	4	452.26	2.50	0.048
INTERACTIONS					
Distance-Power	8,890.71	12	740.89	4.09	0.000
RESIDUAL	18,112.32	100	181.12		

CONCLUSIONS

Two types of longwall air-splitting methods were examined for their dust control performance. These methods included a translucent mesh barrier and a staged spray barrier system to contain the shearer-generated dust along the coal extraction side of the mining face, providing a cleaner split of airflow on the opposing worker walkway side of the mining face. The most effective air-splitting method was the translucent mesh barrier. Both laboratory and underground tests showed that the mesh barrier was quite effective in containing the dust to one side of the entry, provided it was kept relatively parallel to the airflow. Significant dust reductions were achieved in the laboratory up to 61 m downstream of the dust source with two mesh fabrics having material porosities of 52% and 30%. Negligible dust reductions were observed for a more porous mesh

material of 84%. One underground field study verified that the 52% porous mesh provided significant dust reductions at a longwall operation. Dust concentrations were reduced by 53% and 45% at 30 and 60 m inby the shearer, respectively, when the mesh was maintained relatively parallel to the airflow. During support movement the mesh fabric was notably misaligned at the advancing support, negating any dust control effect. Thus, the key factors for controlling dust downstream of the shearer with the translucent mesh barrier are porosity and continuity.

The staged spray barrier system showed marginal dust control effectiveness in the laboratory. The nozzle layout for the staged spray barrier system was developed during preliminary water spray dust control tests. Performance of the spray system was analyzed with respect to the relative fluid power ratio expended between

the spray nozzles and ventilation airflow. The staged spray barrier system was observed to have a limited effective operating range for both water and air-atomized spray nozzles up to 30.5 m downstream of the dust source. During the more extensive air-atomized nozzle experiments, the dust control efficiency of the staged spray barrier system was shown to be negligible beyond 30.5 m downstream of the dust source. The air-atomized nozzles tested significantly reduced the water consumption, but required a compressed air supply to operate the nozzles. Key results from this staged spray barrier research are that the spray power expended must be relatively matched to the ventilation power being used and the downstream dust control effectiveness beyond 30.5 m is insignificant.

The mesh barrier seemed to be the most robust air-splitting method as compared to the staged spray barrier system. The mesh barrier showed significant dust reductions at the farthest downstream distance from the dust source, while operating over a wide range of air velocities. The staged spray barrier system showed a limited range of dust control with respect to spray parameters, ventilation parameters, and downstream distance from the dust source. The spray-to-ventilation power ratio indicates that the spray system would need to be significantly enhanced to control dust on longwalls operating at higher air velocities than those tested. The enhancements required would likely be more closely spaced spray manifolds operated at higher nozzle operating parameters.

Although the mesh barrier seems to be the most promising air-splitting method for longwall dust control, several operational design obstacles need to be overcome for successful integration of this control method into the mining system. The mesh barrier needs low fabric porosity and parallel continuity with airflow to be an effective longwall dust control method. Low fabric porosity would impede worker visibility through the mesh barrier, requiring abundant background lighting on the coal extraction side of the mesh barrier. The lighting requirements may be accomplished either by placing a lighting system on the shearing machine or adding to the existing walkway lighting system used on the supports. Improving the mesh continuity to face airflow would involve removing severe anomalies caused by operational displacements in the mesh. This may be accomplished by hanging the mesh barrier from a supporting framework either affixed to the face conveyor spill plate or anchored periodically among the shield supports. Finally, some additional methane monitoring along the longwall face areas (extraction face and walkway, especially at the longwall gate ends) in gassier coal seams is advisable to ensure that the mesh barrier does not increase methane accumulations along the face.

ACKNOWLEDGMENTS

Research on the staged spray barrier system would not have been possible without the assistance of several of my colleagues at NIOSH's Pittsburgh Research Laboratory (PRL). The author would like to express his appreciation to Thomas Mal, Engineering Technician, for his assistance with the setup, preparation, and execution of these experiments. The author would also like to thank Paul Stefko, Sam Angelo, and Jack Teatino at PRL's Safety Research Coal Mine for their help with the construction of the test section and mine facility support services during these experiments.

REFERENCES

- ASTM, 1996, "ASTM E162-94--Standard Test Method for Surface Flammability of Materials Using a Radiant Heat Energy Source," Annual book of ASTM standards: Vol. 04.07, American Society for Testing and Materials, Conshohocken, PA, pp. 487-497.
- Babbitt, C. and S. Ruggieri, 1990, "Evaluate Fundamental Approaches to Longwall Dust Control Subprogram E - Longwall Application of Ventilation Curtains," USBM Contract Final Report (Contract No. J0318097, Foster-Miller, Inc.), USBM OFR 31E-90, NTIS DE90-015501, 54 pp.
- Bise, C. J., 1986, "Mining Engineering Analysis," Pub. SME, Inc., Littleton, CO., 153 pp.
- Colinet, J. F., E. R. Spencer, and R. A. Jankowski, 1997, "Status of Dust Control Technology on U. S. Longwalls," Proceedings of the 6th international Mine Ventilation Congress, May 17-22, Pittsburgh, PA, Pub. SME, Inc., Littleton, CO, pp. 345-351.
- Haney, R. A., R. S. Ondrey, and K. G. Fields, 1993, "Influence of Airflow and Production on Longwall Dust Control," Proceedings of the 6th U. S. Mine Ventilation Symposium, Salt Lake City, Utah, June 21-23, Pub. SME, Inc., Littleton, CO, pp. 43-49.
- Haney, R. A., 1995, "Trends in Implementation of Longwall Dust Controls," Proceedings of the 7th U.S. Mine Ventilation Symposium, Lexington, KY, June 5-7, Pub. SME, Inc., Littleton, CO, pp. 311-317.
- Hartman, H. L., 1961, "Mine Ventilation and Air Conditioning," John Wiley & Sons, New York, 398 pp.
- Jankowski, R. A., and J. A. Organiscak, and N. I. Jayaraman, 1991, "Dust Sources and Controls for High Tonnage Longwall Faces," Presented at the 120th SME Annual Meeting, Salt Lake City, UT, February 22-26.
- Jankowski, R. A., and J. A. Organiscak, 1983, "Dust Sources and Controls on the Six U. S. Longwalls Having

the Most Difficulty Complying with Dust Standards," USBM Information Circular (IC 8957), 19 pp.
Jayaraman, N. I., R. A. Jankowski, and F. N. Kissell, 1985, "Improved Shearer-Clearer System for Double-Drum Shearers on Longwall Faces," USBM Report of Investigation (RI 8963), 11 pp.

McClelland, J. J., C. Babbitt, and R. A. Jankowski, 1987, "Optimizing Face Ventilation and Shearer Water Consumption to Reduce Longwall Dust Levels," Proceedings of the 3rd Mine Ventilation Symposium, October, 12-14, University Park, PA, Pub. SME, Inc., Littleton, CO, pp. 553-557.

Organiscak, J. A. and M. H. Leon, 1993, "Translucent Face Partition for Longwall Dust Control," Proceedings of the 6th U.S. Mine Ventilation Symposium, Salt Lake City, UT, June 21-23, Pub. SME, Inc., Littleton, CO, pp. 557-562.

Ruggieri, S. K., T. L. Muldoon, W. Schroeder, C. Babbitt, and S. Rajan, 1983, "Optimize Water Sprays for Dust Control on Longwall Shearer Faces," USBM Contract Final Report (Contract No. J0308019, Foster-Miller, Inc.), USBM OFR 42A-86, NTIS PB86-205408, 156 pp.

APPENDIX - FLUID POWER EQUATIONS

(@ standard barometric pressure and air density, from Bise, 1986; Hartman, 1961)

$$\text{POWER RATIO} = \frac{P_{\text{sprays}}}{P_{\text{ventilation}}}$$

Spray Power Equations (P_{sprays})

$$P_{\text{sprays}} = P_{\text{water}} + P_{\text{air}}$$

$$P_{\text{water}} = \frac{8.33 H_w Q_w}{33,000}$$

Where: P_{water} = hydraulic power, horsepower
 H_w = static gage pressure near nozzles, feet of H₂O (velocity pressure negligible below 8 feet per sec of water velocity in pipe)
 Q_w = water quantity, gallon per minute

$$P_{\text{air}} (\text{for } 100 \frac{\text{ft}^3}{\text{min}}) = 1.542 p_1 (r^{0.283} - 1)$$

Where: P_{air} = compressed air power, horsepower
 r = p_2/p_1 , compression ratio
 p_1 = absolute compressor intake pressure, psi
 p_2 = absolute compressor discharge pressure, psi

Ventilation Power Equations ($P_{\text{ventilation}}$)

$$P_{\text{ventilation}} = \frac{5.2 H_v Q_v}{33,000}$$

Where: $P_{\text{ventilation}}$ = ventilation power, horsepower

H_v = ventilation pressure of test section, inches of H₂O
 Q_v = air quantity, cubic feet per minute

$$H_v = H_{\text{static}} + H_{\text{velocity}}$$

$$H_{\text{static}} (\text{for entry airflow}) = H_{\text{loss}} (\text{entry friction loss})$$

$$H_{\text{loss}} = \frac{K L O V^2}{5.2 A} \quad (\text{Atkinson Equation})$$

Where: H_{loss} = energy loss due to friction, inches of H₂O
 K = mine airway friction factor, used 60×10^{-10} for a straight, slightly obstructed sedimentary airway
 L = airway length, feet
 O = airway perimeter, feet
 V = air velocity, feet per minute
 A = airway area, square feet

$$H_{\text{velocity}} = \left(\frac{V}{4,000} \right)^2$$

Where: H_{velocity} = kinetic energy of ventilation, inches of H₂O
 V = air velocity, feet per minute